Modeling of Turbulence and Downbursts for Flight Simulators

Paul A. Robinson* and Lloyd D. Reid†
University of Toronto Institute for Aerospace Studies, Toronto, Ontario, Canada

This study investigates the degree of complexity required in the simulation of turbulence and thunderstorm downbursts for flight simulation. A turbulence model that contains all of the correlations found in homogeneous isotropic turbulence is presented. Several simplifications and alternate models are considered. This paper also presents further developments in the simulation of thunderstorm downbursts. A single ring vortex system, a triple ring vortex system, and Joint Airport Weather Studies (JAWS) data are implemented on the University of Toronto Institute for Aerospace Studies B-747 Flight Simulator. By means of pilot evaluations on this simulator, it was found that the inclusion of the isotropic turbulence correlations did not seem to affect the pilot and not much difference was perceived among the turbulence models. Pilot evaluations of the downburst models showed that both single and triple ring vortex systems produced similar pilot reactions to actual downbursts (JAWS data). It is suggested that the ring vortex models be expanded upon to include more than one downburst cell.

Nomenclature

A = force vector
F = intermittency factor; mean square ratio of analysis of variance
$f(r)$ = longitudinal turbulence correlation
g = gravity vector
$g(r)$ = lateral turbulence correlation
GS_+ = on or above glideslope flight path deterioration parameter (FPDP)
GS_- = below glideslope FPDP
H = aircraft c.g. height above ground
$H_{G/S}$ = glideslope height above ground
j = $\sqrt{-1}$
k = $\sqrt{k_1^2+k_2^2+k_3^2}$ cycles/m
$\boldsymbol{k}$ = wave number expressed in cycles/m: $[k_1 k_2 k_3]^T$
l_h = distance between aircraft c.g. and stabilizer
m = aircraft mass
$\boldsymbol{n}(x)$ = three independent Gaussian white noise sources: $[n_1 n_2 n_3]^T$
$N(k)$ = Fourier transform of $\boldsymbol{n}(x)$
r = $\sqrt{r_1^2+r_2^2+r_3^2}$
r_0 = reference ring vortex radius
$\boldsymbol{r}$ = spatial separation between two points: $[r_1\ r_2\ r_3]^T$
$R_{xx}(\tau)$ = autocorrelation function for $x(t)$ at time delay τ
T_{GS_+} = time spent on or above glideslope
T_{GS_-} = time spent below glideslope
T_{V+} = time spent at or above approach speed
T_{V-} = time spent below approach speed
V = airspeed
$\boldsymbol{V}$ = airspeed vector: $[u_B\ v_B\ w_B]^T$
V_A = approach airspeed, 77 m/s
V_+ = on or above approach speed FPDP
V_- = below approach speed FPDP
$\boldsymbol{W}$ = wind velocity vector: $[W_x\ W_y\ W_z]^T$
δ_{ij} = Kronecker delta
$\sigma(t)$ = modulating variable
σ^2 = turbulence intensity
$\boldsymbol{\Phi}(k)$ = turbulence spectrum function [3 × 3 matrix with elements $\Phi_{ij}(k)$]
Γ_{ref} = reference ring vortex circulation strength
$\tilde{\omega}$ = rotational rate matrix
κ = coefficient of within-pilot consistency

Subscripts
B = body-axes frame of reference
E = inertial frame of reference

Notation
B = matrix
B' = the transpose of $\boldsymbol{B}$
B^* = complex conjugate of $\boldsymbol{B}$
$\dot{V}$ = time derivative of V

Introduction

THE purpose of this paper is to describe several advanced atmospheric models developed for use in flight simulators and to determine, from the reaction of experienced pilots, the fidelity of the models.

Wind shears produced by thunderstorm downbursts have been the cause of several catastrophic aircraft accidents in the past. Although the best strategy for thunderstorm downburst encounters is avoidance, pilots must be trained for the situation of an inadvertent encounter. Training for this type of wind shear encounter can only take place in flight simulators.[1] It is therefore important to evaluate the capability of current atmospheric models to simulate actual occurrences.

Many turbulence models have been proposed in the past and used with varying degrees of success on flight simulators. The effect of spatially correlated gusts and correlated gust components on flight simulation has been of interest for some time.[2] To date, it is not clear whether or not they have an effect on the simulation.

Incorporating Atmospheric Effects in the Flight Equations

The translational equations of motion in the body axes frame, F_B are

$$\dot{V}_{E_B} = A_B/m + g_B - (\tilde{\omega}_B V_{E_B}) \tag{1}$$

where V_{E_B} is the inertial velocity vector in body frame components and

$$\tilde{\omega}_B = \begin{bmatrix} 0 & -r & q \\ r & 0 & -p \\ -q & p & 0 \end{bmatrix}_B \tag{2}$$

Received July 3, 1989; presented as Paper 89-3224 at the AIAA Flight Simulation Technologies Conference, Boston, MA, Aug. 14–16, 1989; revision received Oct. 10, 1989.

*Graduate Student. Member AIAA.
†Professor and Associate Director. Associate Fellow AIAA.

also

$$V_E = V + W \tag{3}$$

$$\Rightarrow \dot{V}_E = \dot{V} + \dot{W} \tag{4}$$

Substituting Eq. (3) and (4) into Eq (1) gives

$$\dot{V}_B = A_B/m + g_B - \dot{W}_B - [\tilde{\omega}_B(V_B + W_B)] \tag{5}$$

The calculation of aerodynamic forces and moments requires the effective rotational motion of the aircraft relative to the air. This is found by

$$\omega_{\text{rel}} = \omega_B - \omega_W \tag{6}$$

The effective rotational rates $\omega_W = [p_G\ q_G\ r_{1_G}\ r_{2_G}]^T$ are related to gradients in the wind field.[3] These gradients and the associated rotational motions are given by

$$p_G = \frac{\partial W_z}{\partial y} \quad q_G = -\frac{\partial W_z}{\partial x} \quad r_{1_G} = -\frac{\partial W_x}{\partial y} \quad r_{2_G} = \frac{\partial W_y}{\partial x} \tag{7}$$

The relative importance of the gradients r_{1_G} and r_{2_G} depend on the configuration of the aircraft. In the case of the Boeing 747 (the aircraft simulated in this work), r_{1_G} is dominant in the calculation of the rolling moment, and r_{2_G} is dominant in the calculation of the yawing moment and side force. These gradients are calculated using the four-point aircraft model described in Ref. 3. The rotational rates are used in Eq. (6) in calculating the aerodynamic forces and moments.

Turbulence Models

Three-Dimensional Correlated and Uncorrelated Models

This section presents a method of generating turbulence with all of the correlations found in homogeneous isotropic turbulence. From the theory of isotropic turbulence, the three-dimensional correlation tensor is[4]

$$R_{ij}(r)/\sigma^2 = [f(r) - g(r)]r_i r_j/r^2 + g(r)\delta_{ij} \tag{8}$$

The Fourier transform of the correlation tensor yields the spectral tensor

$$\Phi_{ij}(\boldsymbol{k}) = \frac{E(k)}{4\pi k^4}(k^2\delta_{ij} - k_i k_j) \tag{9}$$

where $E(k)$ is the von Kármán energy function[5]

$$E(k) = \frac{110}{9}\sigma^2 L \frac{(2\pi aLk)^4}{[1 + (2\pi aLK)^2]^{(17/6)}} \tag{10}$$

Three turbulence velocity components can be generated by

$$\boldsymbol{U}(\boldsymbol{k}) = \boldsymbol{G}(\boldsymbol{k})\ \boldsymbol{N}(\boldsymbol{k}) \tag{11}$$

where $\boldsymbol{U}(\boldsymbol{k})$ and $\boldsymbol{N}(\boldsymbol{k})$ are the Fourier transforms of the turbulence and three independent white noise sources, respectively, and the transfer function $\boldsymbol{G}(\boldsymbol{k})$ comes from the solution to[5]

$$\Phi(\boldsymbol{k}) = \boldsymbol{G}^*(\boldsymbol{k})\ \boldsymbol{G}'(\boldsymbol{k}) \tag{12}$$

The inverse Fourier transform of $\boldsymbol{U}(\boldsymbol{k})$ produces the spatial turbulence velocity field $\boldsymbol{u}(\boldsymbol{r})$. This model assumes Taylor's hypothesis of a frozen flowfield.[5]

There are two possible formulations of the transfer function matrix $\boldsymbol{G}(\boldsymbol{k})$. If $\boldsymbol{G}(\boldsymbol{k})$ is taken to be

$$\boldsymbol{G} = \begin{bmatrix} G_{11} & 0 & 0 \\ G_{21} & G_{22} & 0 \\ G_{31} & G_{32} & G_{33} \end{bmatrix} \tag{13}$$

the resulting three components of the velocity field $\boldsymbol{u}(\boldsymbol{r})$ will be correlated with each other according to Eq. (8). Alternatively, $\boldsymbol{G}(\boldsymbol{k})$ can be taken as

$$\boldsymbol{G} = \begin{bmatrix} G_{11} & 0 & 0 \\ 0 & G_{22} & 0 \\ 0 & 0 & G_{33} \end{bmatrix} \tag{14}$$

This results in the three components being independent of each other. The latter is the formulation employed in Ref. 6.

The aforementioned procedure produces two separate models. Throughout this work, the turbulence produced by the formulation in Eq. (13) will be referred to as the three-dimensional correlated turbulence model and that produced by Eq. (14) as the three-dimensional uncorrelated model. It should be borne in mind, however, that both models contain the spatial correlations found in isotropic turbulence.

As the aircraft flies through this field, the turbulence velocity components at its c.g. are determined and transformed from the gound-fixed F_E frame into the aircraft body frame F_B. In a similar manner, the significant turbulence velocity gradients [Eq. (7)] are computed in F_B as well. This generates a turbulence time series consisting of three turbulence velocities ($u_G\ v_G\ w_G$) and the four gradients from Eq. (7) ($p_G\ q_G\ r_{1_G}\ r_{2_G}$), which are used to produce aircraft forces and moments. Also, the wind components and their time derivatives are included in Eq. (5).

It is generally accepted that turbulence is a non-Gaussian process.[7] The amplitude distribution tends to be patchy, with significant periods of low and high intensity. This property requires that the probability density function of the gust velocities be other than Gaussian, the primary difference being in the kurtosis, the ratio of the fourth-order moment to the square of the second-order moment. The method of producing the turbulence just described was based on the filtering of Gaussian white noise and, as a consequence, the turbulence field was also Gaussian. In order to increase the realism in flight simulation applications, it is necessary to alter the statistical properties of this initial turbulence while maintaining the spectral characteristics. A suitable process has been introduced in Ref. 8 and is given by

$$w(t) = \sigma(t)\ z(t) \tag{15}$$

where it is desired to have the spectral properties of some time series $w(t)$ identical to those of $z(t)$ and at the same time to have a different probability density function. This is achieved by employing a stochastically fluctuating $\sigma(t)$. It can be shown that the desired properties can be achieved when

$$\frac{\mathrm{d}^2 R_{\sigma\sigma}(\tau)}{\mathrm{d}\tau^2} \tag{16}$$

is suitably small as $\tau \to 0$. This technique has been used in this study to process the turbulence field in order to generate patchy turbulence. At each time step a new value of $\sigma(t)$ is calculated, and this value is used to modulate the turbulence gusts u_G, v_G, w_G, p_G, q_G, r_{1_G}, and r_{2_G}.

Modulated Turbulence Model

The preceding models require the turbulence to be generated in the frequency domain. Alternatively, by filtering white noise using simple linear filters turbulence may be generated in the time domain. In the past, much attention has been focused on the three-filter turbulence generation models proposed in Refs. 7, 9, and 10. The modulated turbulence model is an adaptation of the three-filter model, but instead of using three filters to produce a patchy time series, the preceding modulation process [Eq. (15)] is used, reducing the number of filters required for each gust series to one. The u_G, v_G and w_G gusts are generated with the Dryden spectral forms,[11] and rolling and yawing gusts (p_G and r_{1_G}, respectively) are generated using filters with transfer functions based on Ref. 10. Pitch gusts are produced by applying a time delay to the α_G at the aircraft c.g. and applying it to the stabilizer as described in Ref. 10, i.e.,

$$\alpha_{G\text{stab}}(t) = \alpha_{G\text{c.g.}}\,[t - (l_h/V)] \tag{17}$$

All of the linear filters are driven by Gaussian white noise sources. These sources are statistically independent, the u_G and r_{1_G} filters sharing the same source, and the w_G and p_G filters sharing their own source. All gusts u_G, v_G, w_G, p_G, and r_{1G} are multiplied by a suitable stochastic $\sigma(t)$ function to generate the required statistical properties. All gust components use the same value of $\sigma(t)$.

The method of implementation is taken to be that described in the literature describing this model.[10] The gusts just described are incorporated in Eqs. (1) and (3) as described earlier. This model differs from the pair of three-dimensional models in that the Dryden spectral form is employed. Also the turbulence from this model is not restricted to the spatial or component correlations found in the first two models.

Statistical Discrete Gust Method

As a fourth model, a very different approach to generating turbulence is employed. Developed at the Royal Aircraft Establishment, the statistical discrete gust (SDG) method uses as a basic element a ramp gust followed by an exponential washout.[12-14] The exact procedure for generating the turbulence is given in Ref. 12. The u_G, v_G, and w_G gusts are generated at the aircraft's c.g. as in the previous models. Roll and yaw gusts (p_G and r_{1_G}, respectively) are calculated by generating w_G and u_G gusts independently at each wingtip and dividing the difference by the separation distance [Eq. (7)]. Pitch gusts were generated using the time delay process of Eq. (17). As with the modulated turbulence model in the previous section, the gusts were implemented using Eq. (1) and (3).

The preceding four turbulence models represent three very different methods of generating turbulence for flight simulators. The variation of turbulence intensities and lengthscales with height was according to the data in Ref. 16. In order to generate the patchy nature of turbulence, the fourth-order central moment of all of the gusts series was set to give a kurtosis of 5. This value was chosen as a realistic value for the local wind conditions.[15] To produce the kurtosis in the SDG model, the intermittency factor F was set at 0.4.[12] During the turbulence evaluations detailed below, the surface wind speed was on a reciprocal heading to the runway at 8 m/s 10 m above ground. The mean wind variation with height was according to the power law given in Ref. 16.

By means of pilot evaluations, the realism of each model and its value in a piloted flight simulation can be examined.

Thunderstorm Downburst Modeling

In recent years, increasing emphasis has been placed on training airline pilots for flight through wind shear conditions. Several downburst models for flight simulators have been proposed in the past using elements of potential flow theory to simulate the velocity field.[17-19] Such models have been shown capable of producing aircraft response similar to that observed in real encounters. However, a direct comparison on the basis of pilot evaluations between these models and actual downbursts has not been undertaken in the past. Such a comparison could not be made until results such as those from the Joint Airport Weather Studies (JAWS) were made available for simulation applications.[20] This allowed direct comparison between the simpler models and the larger JAWS data sets.

In Ref. 18, it is suggested that a downburst model using a single ring vortex (and its image) will not produce a realistic wind field; in particular, the ratio of the maximum vertical wind speed to the maximum horizontal wind field would be too small in the single ring case. It is suggested that several concentric ring vortices of different strengths be employed to

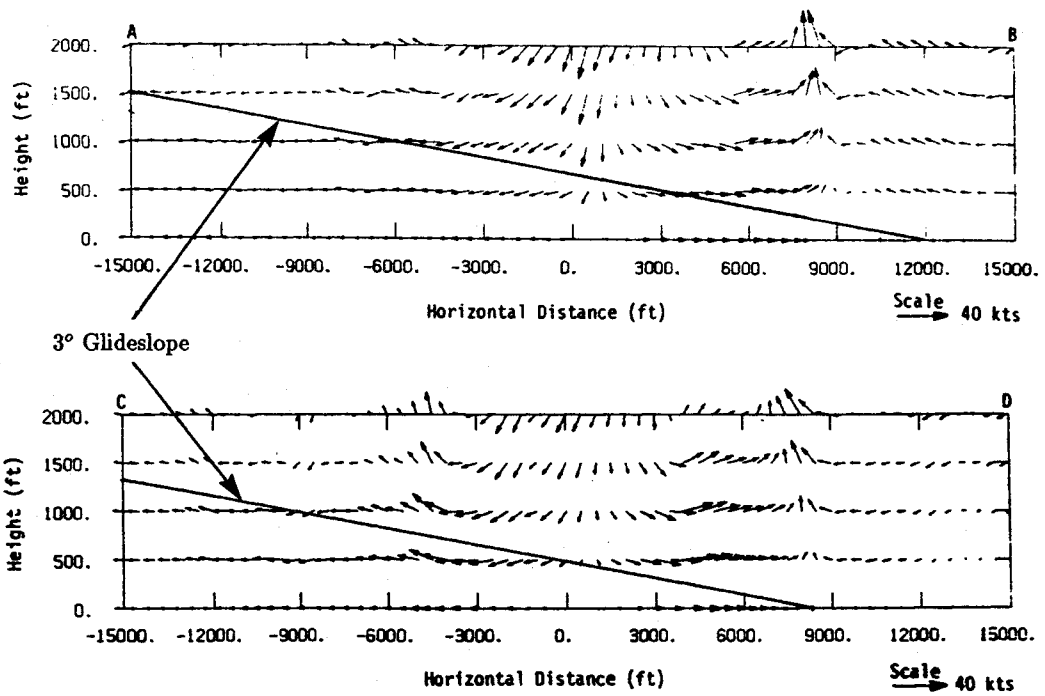

Fig. 1 JAWS corridors AB and CD.[20]

obtain a more realistic profile. Strengths would increase toward the center to produce a more intense, localized downdraft. Two models were studied in this work. The first employs a single ring vortex and the second uses three concentric ring vortices of radii r_i, with a strength distribution given by

$$\Gamma_i = \Gamma_{\text{ref}}\left[1 - \sin\left(\frac{\pi}{2}\frac{r_i}{r_0}\right)\right] \qquad i = 1,2,3 \tag{18}$$

with $r_{1,2,3} = 0.75r_0$, $0.5\,r_0$, and $0.25r_0$, respectively. The models were implemented in such a way that both required equal computation time in the simulation, thereby removing a common argument against the more complicated models in the past. This was achieved by using look-up tables of velocities generated offline.

Two data sets were selected from the JAWS data in Ref. 20: corridors AB and CD from data set 5AU1847. Vertical cross-sections of these downbursts are shown in Fig. 1,[20] as well as the orientation of the ILS 3-deg glideslope used in these evaluations. The arrows in the figure represent the wind velocity vector at a point. These downbursts were measured in the atmosphere using triple Doppler radar. The spatial resolution of the measurements was 150 m. These particular downburst profiles were chosen as they had already been classified as challenging[20] and consisted of one well-defined downburst but having different vertical wind structures. The single and triple ring models' parameters were adjusted in such a way that both generated wind components along the glideslope as close as possible to those generated by the JAWS data sets. This gave rise to six separate wind shear sets. Since there is no turbulence information in the JAWS data sets, none of the wind shears contained any turbulence.

Experimental Design

All of the preceding models were implemented on the University of Toronto Institute for Aerospace Studies (UTIAS) Flight Simulator shown in Fig. 2. The aircraft simulated was a Boeing 747. The aircraft weight was set at 226,800 kg (500,000 lb). This aircraft represents one of the larger commercial types in service, both in terms of weight and spatial dimensions. Its wing loading in the simulation is comparable to that of many different commercial jets in service today. The results of these evaluations will be applicable mainly to commercial aircraft of similar dimensions and wing loading. Details of the simulator can be found in Refs. 21–23. The simulator was upgraded from that described in Ref. 21 to include a three-window color visual display and a hydraulic control loading system.

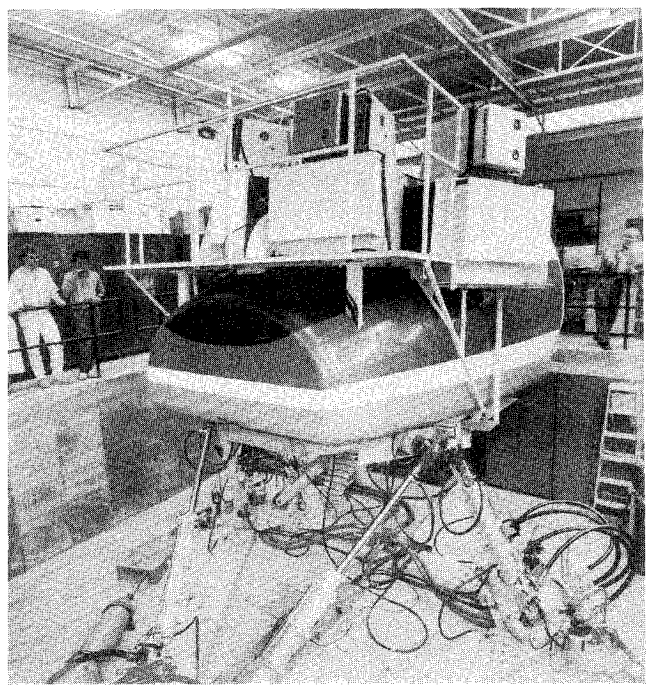

Fig. 2 UTIAS flight research simulator.

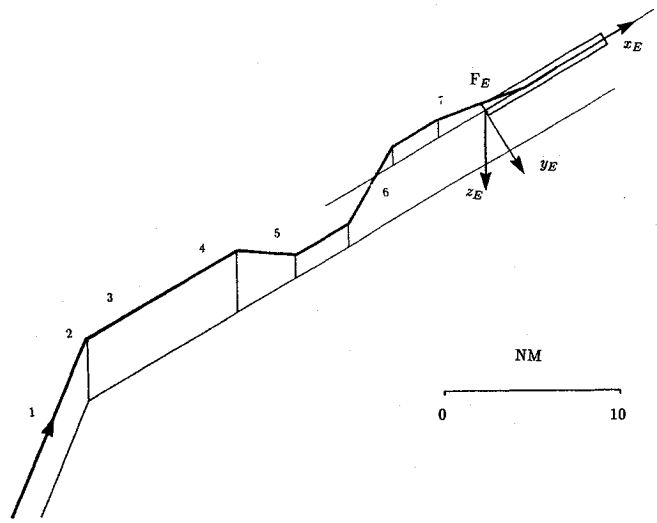

Fig. 3 Primary task in turbulence evaluations.

In order to evaluate the turbulence and downburst models, use was made of current airline pilots. All pilots had experience in training simulators. In all, six pilots were employed for the turbulence evaluations and six for the downburst tests. Although only one had Boeing 747 experience, the pilots were given sufficient training such that useful results could be obtained from all of them.

Turbulence Evaluations

The object of the turbulence evaluations was to determine what aspects of turbulence modeling are important in producing a simulation perceived as realistic by pilots.

The task used in the turbulence evaluations is very similar to that used in Ref. 21, namely to perform a landing approach as shown in Fig. 3. It was selected to present the terminal portion of a flight and comprises the following zones: 1) Heading and altitude hold; 2) VOR radial intercept; 3) VOR radial track; 4) deceleration while tracking VOR radial; 5) descent; 6) sidestep maneuver to capture the ILS; and 7) ILS approach to touchdown. The pilots were instructed to judge the quality of the atmospheric model and no other aspect of the simulation. It was also made clear that they should rate the models relative to that which would be experienced in the actual aircraft they fly in service and not in other simulators.

Both subjective and objective measurements were used to evaluate the effects of the turbulence models. The subjective ratings used the scale shown in Fig. 4. The rating scale is based on that reported in Refs. 21 and 24, and the adjectives on the left-hand side are spaced so as to produce an equal interval scale. Interval data is obtained using a continuous numerical scale (1–10) shown on the right-hand side of Fig. 4. In addition, the pilots were encouraged to add any comments they wished. Immediately after each trial, the pilots were asked to mark on each vertical line their assessment of the turbulence. The pilot flew the full task (Fig. 3) for each turbulence model (in a randomized order) and once with no turbulence. No ratings were taken for the latter case. In addition to this, the pilots flew paired comparison tests. This allowed the pilots to compare the turbulence models to each other and obtain a ranking of the models in order of preference. The paired comparison tests were carried out in zone 7 and took about 4 min to fly. A single trial consisted of flying the particular task twice in close succession but with different turbulence models.

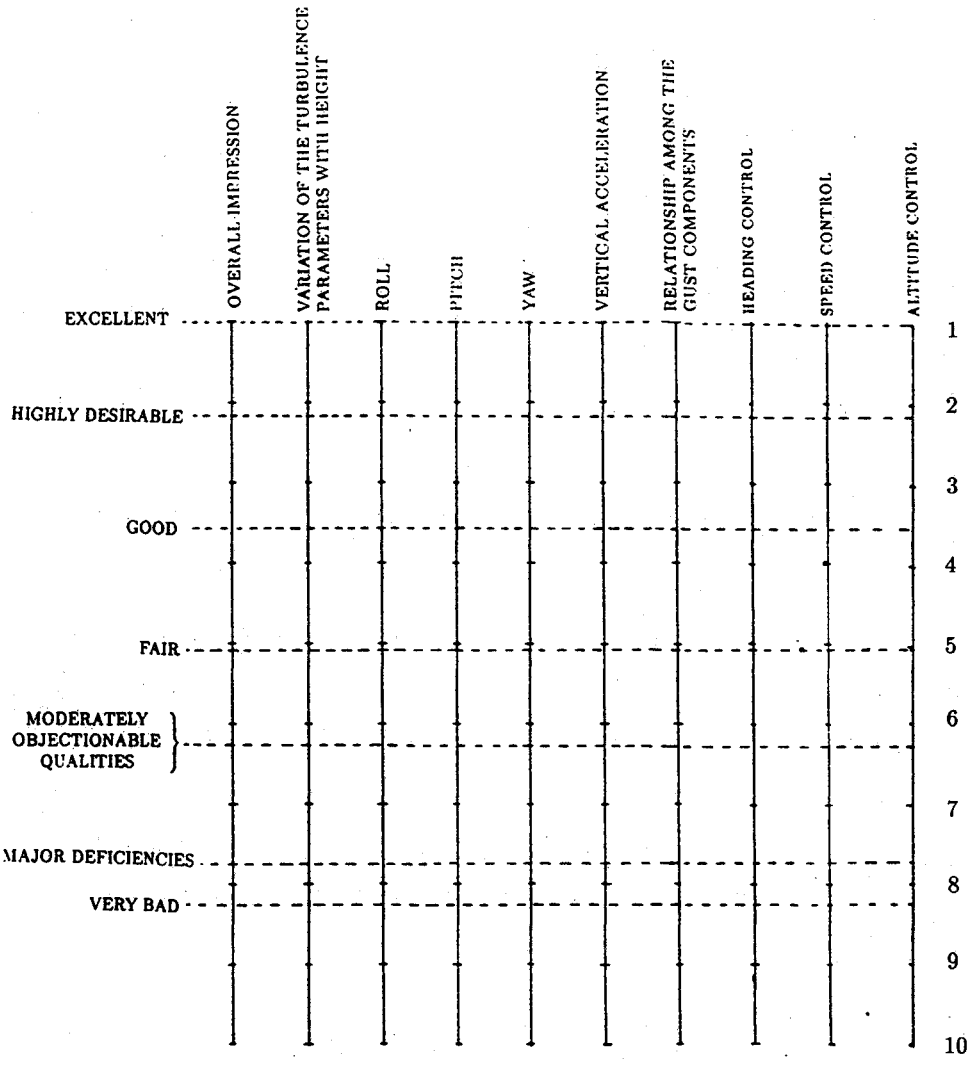

Fig. 4 Pilot rating scales.

After flying each pair, the pilot was asked to indicate which model was more realistic. All possible pairs were presented to the pilot in a randomized Latin-Square order.

Downburst Evaluations

The purpose of the downburst evaluations was to examine whether the ring vortex models could produce pilot and aircraft responses similar to those produced by the JAWS data sets and, if so, whether a single ring vortex model is sufficient or a more complicated model is required. No attempt was made to provide training in flight through the wind shear, the pilots already having received this background as part of their service training. These evaluations are of the wind models and not the pilots' training. It is also of interest to determine if any improvement in the pilots' performance takes place over the course of the evaluations, for although no training was provided, the pilots may learn from one run to the next, thus improving their performance.

The downburst evaluations required the pilots to fly an approach to land (zone 7). They were asked to fly the approach to the best of their ability, and to go-around only when a landing seemed impossible. On landing, brakes were applied to a full stop. The decision to go-around and the procedures used were at the discretion of the pilot. In all cases, the procedure learned in their previous training was to apply full throttle, pitch up to the stick-shaker warning, and not alter the aircraft configuration until clear of the perceived danger. During the tests, they were given no instruction in how to fly the various shears or recovery procedures.

Results and Analysis

Turbulence Evaluations

The pilot sample size was six. The number of pilots was constrained by the minimum required for the paired comparison tests (six in this case) and the availability of pilots to take part. Means and standard deviations were calculated for control inputs, airspeed, aircraft position, Euler angles, and angular rates. In the following discussion each turbulence model will be referred to as follows: 1) M1—modulated turbulence model; 2) M2—statistical discrete gust model; 3) M3—three-dimensional uncorrelated model; 4) M4—three-dimensional correlated model; 5) NT—no turbulence.

A one-sided analysis of variance was carried out on the turbulence evaluation results. In the discussion that follows, subject effects are those attributed between the pilots, treatment effects are those attributed between the turbulence models, and scale effects are those attributed between the rating scales in Fig. 4. The parameter $P(x>F)\%$ represents the significance of the test as a probability between 0 and 100%. Values from 0 to 2.5% are taken as representing very significant trends in the data, 2.5 to 5% as significant and 5 to 10% as mildly significant.

Pilot Ratings

Separate analyses of variance were calculated on each of the rating scales (i.e., column headings in Fig. 4). A sample summary table is shown in Table 1 and an overall summary of the results is given in Table 2. These results are calculated exclud-

Table 1: Sample table from the analysis of variance for the "overall impression" rating scale: without NT data

Effect[a]	Deg of freedom	Sum of squares	Mean square	F value	$P(x>F)\%$
Subjects	5	12.0933	2.4187	1.5537	23.3
Treatments	3	9.0300	3.0100	1.9336	16.8
Residual	15	23.3500	1.5567		
Total	23	44.4733			

[a]"Treatments" refers to the four turbulence models.

Table 2 Analysis of variance summary of turbulence evaluations; $P(x>F)\%$

Rating	Subjects	Treatments
Overall impression	23.3	16.8
Variation of turbulence parameters with height	0.4	21.2
Roll realism	15.1	5.9
Pitch realsim	0.2	2.9
Yaw realism	6.6	12.1
Vertical acceleration	1.5	1.9
Relation between gust components	16.0	1.7
Heading control	7.5	2.8
Speed control	1.6	3.3
Altitude control	3.5	16.7

ing the NT data. It can be seen that subject effects are most significant for the "variation of the turbulence parameters with height" and the "pitch realism" parameters. The pilots consistently marked model M2 lower than the other models on all of the rating scales. This accounts for the level of significance of the treatment effects as there was not very much difference between the ratings for the other three models.

Pilot Performance and Aircraft Response

Measurements of the pilots' control activity and the aircraft's state variables were made. The means and standard deviations were calculated for each parameter. Also an analysis of variance was carried out on each parameter (excluding the NT data). From these results several observations can be made. Model M2 produced the largest flight path deviations overall; however, there was no well-defined difference in the aircraft response or pilot performace among the other three turbulence models. It was found that the method of implementing pitch gusts in models M1 and M2 [using the α time delay in Eq. (17)] produced large pitch deviations. Such motions were found to be unrealistic and a major source of altitude departures. This would indicate that this method of generating pitch gusts is unacceptable. It was found that in the early part of the task (up to the descent), M2 produced the largest standard deviation of control inputs (on all axes) and was found to be unrealistically harsh. On the approach, it was found that models M3 and M4 produced larger indicated airspeed fluctuations than the other two models. This resulted in slightly larger throttle activity on the part of the pilots.

Paired Comparison Tests

In these test, pilots were asked to compare the four turbulence models over a short flight segment. Each of the six pairs were flown by the pilot according to a Latin-Square order. For each pilot, a ranking of the models in order of perceived realism was obtained. In addition, an overall ranking was obtained. The analysis is described in detail in Ref. 25. In calculating the overall rankings, it is possible to judge the within-pilot and interpilot consistency. The first will judge whether the pilot ranked the four models consistently, in which case the coefficient of within-pilot consistency κ will be 1, or in a completely radom fashion, where κ will be 0. Inconsistency arises from pilots judging model 1 better than model 2, model 2 better than model 3, and model 3 better than model 1, for example. Also the coefficient of interpilot consistency W can be calculated. A value of W of 1 indicates complete consistency and agreement among the pilots and a value of 0 indicates completely random order among the pilots. The segment chosen was the ILS approach to touchdown (zone 7). The results are shown in Table 3. From the analysis, the pilots preferred model M1 overall. However, the within-pilot consistency κ was low for some pilots. As a consequence of the poor within-pilot consistency, the interpilot consistency W was also low for both segments.

Thunderstorm Downburst Wind Shear Evaluations

Six pilots were employed in the downburst evaluations. In studying the pilots performance in flying through the thunderstorm wind shears, two aspects are examined: First, whether the ring vortex models produce similar pilot and aircraft responses to those due to the JAWS data sets, and second, whether there is any noticeable improvement in the pilots' performance over the course of the evaluations.

In the course of the discussion the wind shears will be referred to as follows: 1) J1—JAWS AB corridor data set; 2) SR1—single ring vortex model simulation of JAWS AB corridor; 3) TR1—triple ring vortex model simulation of JAWS AB corridor; 4) J2—JAWS CD corridor data set; 5) SR2—single ring vortex model simulation of JAWS CD corridor; 6) TR2—triple ring vortex model simulation of JAWS CD corridor; 7) NS—no shear.

A similar analysis to that of the approach phase of the turbulence evaluations was carried out. That is, the means and standard deviations of the control inputs and aircraft state variables were calculated and an analysis of variance was applied. In addition, several FPDPs were calculated. These are similar to those in Ref. 26. Those used in this work are defined as follows:

$$GS_+ = \frac{1}{T_{GS_+}} \int_0^{TG_{S+}} \frac{H}{H_{G/S}}\,dt \tag{19}$$

$$GS_- = \frac{1}{T_{GS_-}} \int_0^{TG_{S-}} \frac{H}{H_{G/S}}\,dt \tag{20}$$

$$V_+ = \frac{1}{T_{V_+}} \int_0^{TV+} (V - V_A)\,dt \text{ [m/s]} \tag{21}$$

$$V_- = \frac{1}{T_{V_-}} \int_0^{TV-} (V - V_A)\,dt \text{ [m/s]} \tag{22}$$

Table 3 Summary of turbulence evaluation paired comparison tests

Rating (best → worst)	κ	W
M1-M3-M2-M4	(1.0,0.5,1.0,0.5,1.0,1.0)	0.122

The increasing headwind experienced by an aircraft approaching a thunderstorm downburst causes its airspeed to increase, and the consequent increase in lift leads to the aircraft rising above the glideslope. In an effort to attain a stabilized approach, half of the subject pilots during their initial runs, in finding themselves above the glideslope for a given power setting, surprisingly interpreted (through comments after each flight) the wind profile as an increasing tailwind. This was because they found themselves above the glideslope for a given power setting and glideslope angle and perceived this as being convected by a tailwind. It was not until they had encountered the downdraft that they understood the nature of the wind field through which they were flying. This observation emphasizes the insidious nature of the downburst wind shear.

The capability of the ring vortex models to simulate the JAWS wind field was examined. Figure 5 shows that FPDPs GS_+ and GS_- were reproduced well in both AB and CD cases for all ring vortex models. During the course of the tests, it was observed that the pilots' primary task on encountering the shear was to avoid undershooting the approach; airspeed only becoming a primary consideration as it approached the stall speed. Consequently, the primary indicators of the effect of the shear should be the glideslope and velocity FPDPs GS_+, GS_-, V_+, V_-. Figure 5 shows these parameters averaged over all the pilots' results. It can be seen that all six wind shear models produce very similar GS_+ values, with very little spread in the SR2 and TR2 models. For the GS_- values, the SR2 model has the greatest spread. The V_+ parameter is produced equally well for the three _1 models, with some variation in the _2 models. Similarly for V_-, with TR2 producing the largest airspeed loss value.

In comparing the overall results from the single ring and triple ring vortex modes, it was found that the single ring model produced results closer to those from the CD corridor and the triple ring closer to those from the AB corridor. This would suggest that both forms produce downburst flowfields similar to those observed in the atmosphere.

Although the tests are not exhaustive, it may be understood from these results that the wind velocity field due to a thunderstorm downburst may be modeled using a ring vortex system, thus avoiding the use of larger, less flexible data sets. The wind shears used in these tests were all found by the pilots to be realistic. However, the results presented pertain only to a very short portion of the flight phase. Exposing a pilot in a simulator to one single downburst cell may evoke a false sense of security, in that once a go-around, should it be required, has been initiated and the perceived threat cleared, the pilot will be safe. In reality however, several downburst cells have been observed to exist simultaneously in very close aproximity, and in clearing one cell the pilot may inadvertently fly into another. A combination of cells would therefore be desirable. The method of implementation of the ring vortex models used in this work is such that several cells may be included without very much increase in computation time. However, the ability to use only a single cell may enhance the use of the ring vortex models as a training tool, allowing the pilot practice in the basic recovery procedures before tackling more taxing scenarios.

In examining the variation of each parameter studied over the course of the six runs (seven including the no-shear data) averaged over the six pilots, there was not found to be an significant change between the performance in the first run or the last. A similar result was found when the pilots' results were analyzed separately. It is thought that the statistical population and the sample sizes are too small to indicate any learning trend.

Conclusions and Recommendations

It was found that the pilots could not discern between the turbulence models in their subjective ratings. There did not seem to be any appreciable difference in the pilots' performance, or aircraft response between the formulations of models M3 and M4 [Eqs. (13) and (14)]. The inclusion of spatial correlations in the turbulence models did not seem to have a significant effect on the pilot or the aircraft. Also, without some modification, the pitch gusts generated using Eq. (17) were excessive and unrealistic. Although this method has been used in studies in the past, it does not seem to be an acceptable method of producing pitch gusts. Any future modification to this method may have to take into account the wing downwash.

The downburst evaluations revealed the ring vortex models to be very capable in simulating the JAWS data. Both ring

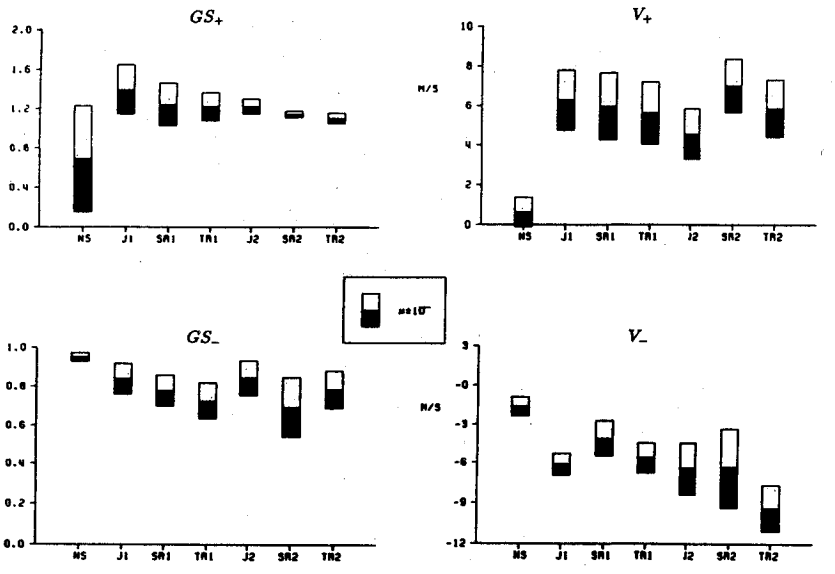

Fig. 5 FPDPs for downburst models.

vortex models produced results comparable to those from observed downbursts, implying that such models may be employed in the future as useful training tools. Further research should be carried out in defining realistic boundaries for the various ring vortex model parameters: strength, radius, height, and tilt. Also several ring vortex systems may be combined to make a larger, more complex flowfield. This can be done without an excessive computational overhead. Finally, further study should be made in implementing a turbulence structure in the ring vortex flowfield. Although turbulence models have been included with such models in the past,[19] they have been simply superimposed on the flowfield. Previous work[27] indicates that there is a complicated turbulence structure associated with the downburst and its associated gust front.

Acknowledgments

The authors would like to thank the evaluation pilots who took part in the project. They were unpaid volunteers who displayed a high degree of interest and professionalism throughout the experiments. Without their expertise and dedication, this study could not have been completed. The authors also wish to thank the staff at the Canadian Airlines Pilots Association, Air Canada, and Boeing Canada for their help in recruiting the pilots. The financial support of the Natural Sciences and Engineering Research Council of Canada is gratefully acknowledged.

References

[1]"Airborne Low Altitude Wind Shear Equipment and Training Requirements; Final Rule," U.S. Dept. of Transportation (FAA) 14 CFR parts 121 and 135, Docket No. 19110, Ammend. Nos. 121-199, 135-127.

[2]Houbolt, J. C., "Survey on Effect of Surface Winds on Aircraft Design and Operation and Recommendations for Needed Wind Research," NASA CR-2360, Dec. 1973.

[3]Etkin, B., "The Turbulent Wind and its Effect on Flight," AIAA Wright Brothers Lecture, *UTIAS Review 44,* Aug. 1980.

[4]Batchelor, G. K., *Homogeneous Turbulence*, Cambridge Univ., Cambridge, England, 1953.

[5]Etkin, B., *Dynamics of Atmospheric Flight*, Wiley, New York, 1972.

[6]Campbell, C. W., "A Spatial Model of Wind Shear and Turbulence for Flight Simulation," NASA TP-2313, May 1984.

[7]Van de Moesdjk, G. A. J., "Non-Gaussian Structure of the Simulated Turbulent Environment in Piloted Flight Simulation," Dept. of Aerospace Engineering, Delft University of Technology, The Netherlands, Memo M-304, April 1978.

[8]Press, H., "Atmospheric Turbulence Environment with Special Reference to Continuous Turbulence," AGARD Report 115, April -May 1957.

[9]Reeves, P. M., "A Non-Gaussian Turbulence Simulation," USAF AFFDL-TR-69-67, Nov. 1969.

[10]Van de Moesdijk, G. A. J., "Specification of a Non-Gaussian Turbulence Model for On-Line Flight Simulation," Fokker, the Netherlands, Rept. A161, May 1985.

[11]Dryden, H. L., "A Review of the Statistical Theory of Turbulence," *Quarterly of Applied Mathematics 1943-45*, Jan. 1943.

[12]Tomlinson, B. N., "Developments in the Simulation of Atmospheric Turbulence," Royal Aeronautical Establishment TM FS-46, Sept. 1975.

[13]Jewell, W. F., and Heffley, R. K., "A Study of the Key Features of the RAE Atmospheric Turbulence Model," NASA CR-152194, Oct. 1978.

[14]Jones, J. G., "Review of Atmospheric Structures and Models. A Statistical Discrete Gust Theory Progress Note," Royal Aircraft Establishment TM FS-186, June 1978.

[15]Dutton, J. A., and Deaven, D. G., "Some Observed Properties of Atmospheric Turbulence," *Statistical Models and Turbulence Lecture Notes in Physics*, Springer-Verlag, New York, 1972.

[16]Items 72026, 74030, 74031, and 75001, Engineering Sciences Data Unit, London, England.

[17]Zhu, S., and Etkin, B., "Fluid Dynamic Model of a Downburst," University of Toronto Institute of Aerospace Studies, Toronto, Rept. 271, April 1983.

[18]Bray, R. S., "A Method for Three-Dimensional Modeling of Wind Shear Environments for Flight Simulator Applications," NASA TM-85969, July 1984.

[19]Woodfield, A. A., "Real-Time Simulation of Thunderstorm Wind Shear, Turbulence, and Steady Wind," Royal Aircraft Establishment, Bedford, U.K., 1984.

[20]Frost, W., Chang, H. P., Elmore, K. L., and McCarthy, J., "Microburst Wind Shear Models from Joint Airport Weather Studies," Dept. of Transportation/Federal Aviation Adminisration, PM-85-18, June 1985.

[21]Reid, L. D., and Nahon, M. A., "Flight Simulation Motion-Base Drive Algorithms: Part 3—Pilot Evaluations," University of Toronto, Institute of Aerospace Studies, Toronto, Canada, Rept. 319, Dec. 1986.

[22]Hanke, C. R., and Nordwall, D. R., "The Simulation of a Jumbo Jet Transport Aircraft, Volume 2: Modeling Data," NASA CR-114494, Sept. 1970.

[23]Hanke, C. R., "The Simulation of a Large Jet Transport Aircraft," NASA CR-1756, March 1971.

[24]McDonnell, J. D., "An Application of Measurement Methods to Improve the Quantitative Nature of Pilot Rating Scales," *IEEE Transactions on Man-Machine Systems*, Vol. MMS-10, No. 3, 1969, pp. 81-92.

[25]Seaver, D.A., and Stillwell, W. G., "Procedures for Using Expert Judgement to Estimate Error Probabilities in Nuclear Power Plant Operations," U.S. Nuclear Regulatory Commission, CR-2743, pp. A-1-A-12.

[26]Frost, W., Turkel, B. S., and McCarthy, J., "Simulation of Phugoid Excitation Due to Hazardous Wind Shear," AIAA Paper 82-0215, Jan. 1982.

[27]Lewellen, W. S., Teske, M. E., and Seguar, H., "Turbulence Transport Model of Wind Shear in Thunderstorm Gust Fronts and Warm Fronts," NASA CR-3002, May 1978.